



**AUTHOR(S):**

**TITLE:**

**YEAR:**

**Publisher citation:**

**OpenAIR citation:**

**Publisher copyright statement:**

This is the \_\_\_\_\_ version of an article originally published by \_\_\_\_\_  
in \_\_\_\_\_  
(ISSN \_\_\_\_\_; eISSN \_\_\_\_\_).

**OpenAIR takedown statement:**

Section 6 of the "Repository policy for OpenAIR @ RGU" (available from <http://www.rgu.ac.uk/staff-and-current-students/library/library-policies/repository-policies>) provides guidance on the criteria under which RGU will consider withdrawing material from OpenAIR. If you believe that this item is subject to any of these criteria, or for any other reason should not be held on OpenAIR, then please contact [openair-help@rgu.ac.uk](mailto:openair-help@rgu.ac.uk) with the details of the item and the nature of your complaint.

This publication is distributed under a CC \_\_\_\_\_ license.

\_\_\_\_\_

## Accepted Manuscript

Title: Enhancing photocatalytic degradation of the cyanotoxin microcystin-LR with the addition of sulfate-radical generating oxidants

Authors: M.G. Antoniou, I. Boraie, M. Solakidou, Y. Deligiannakis, M. Abhishek, L.A. Lawton, C. Edwards



PII: S0304-3894(18)30671-X  
DOI: <https://doi.org/10.1016/j.jhazmat.2018.07.111>  
Reference: HAZMAT 19620

To appear in: *Journal of Hazardous Materials*

Received date: 4-4-2018  
Revised date: 9-7-2018  
Accepted date: 30-7-2018

Please cite this article as: Antoniou MG, Boraie I, Solakidou M, Deligiannakis Y, Abhishek M, Lawton LA, Edwards C, Enhancing photocatalytic degradation of the cyanotoxin microcystin-LR with the addition of sulfate-radical generating oxidants, *Journal of Hazardous Materials* (2018), <https://doi.org/10.1016/j.jhazmat.2018.07.111>

This is a PDF file of an unedited manuscript that has been accepted for publication. As a service to our customers we are providing this early version of the manuscript. The manuscript will undergo copyediting, typesetting, and review of the resulting proof before it is published in its final form. Please note that during the production process errors may be discovered which could affect the content, and all legal disclaimers that apply to the journal pertain.

Revised for Publication in

**Journal of Hazardous Materials**

July 2018

# Enhancing photocatalytic degradation of the cyanotoxin microcystin-LR with the addition of sulfate-radical generating oxidants

*M.G. Antoniou<sup>1,\*</sup>, I. Boraei<sup>1</sup>, M. Solakidou<sup>2</sup>, Y. Deligiannakis<sup>3</sup>, M. Abhishek<sup>4</sup>, L.A. Lawton<sup>4</sup>, and C. Edwards<sup>4</sup>*

*<sup>1</sup>Department of Environmental Science and Technology, Cyprus University of Technology, 3036 Lemesos, Cyprus*

*<sup>2</sup>Laboratory of Biomimetic Catalysis and Hybrid Materials, Department of Chemistry, University of Ioannina, 45110, Ioannina, Greece*

*<sup>3</sup>Laboratory of Physical Chemistry of Materials and Environment, Department of Physics, University of Ioannina, 45110 Ioannina, Greece*

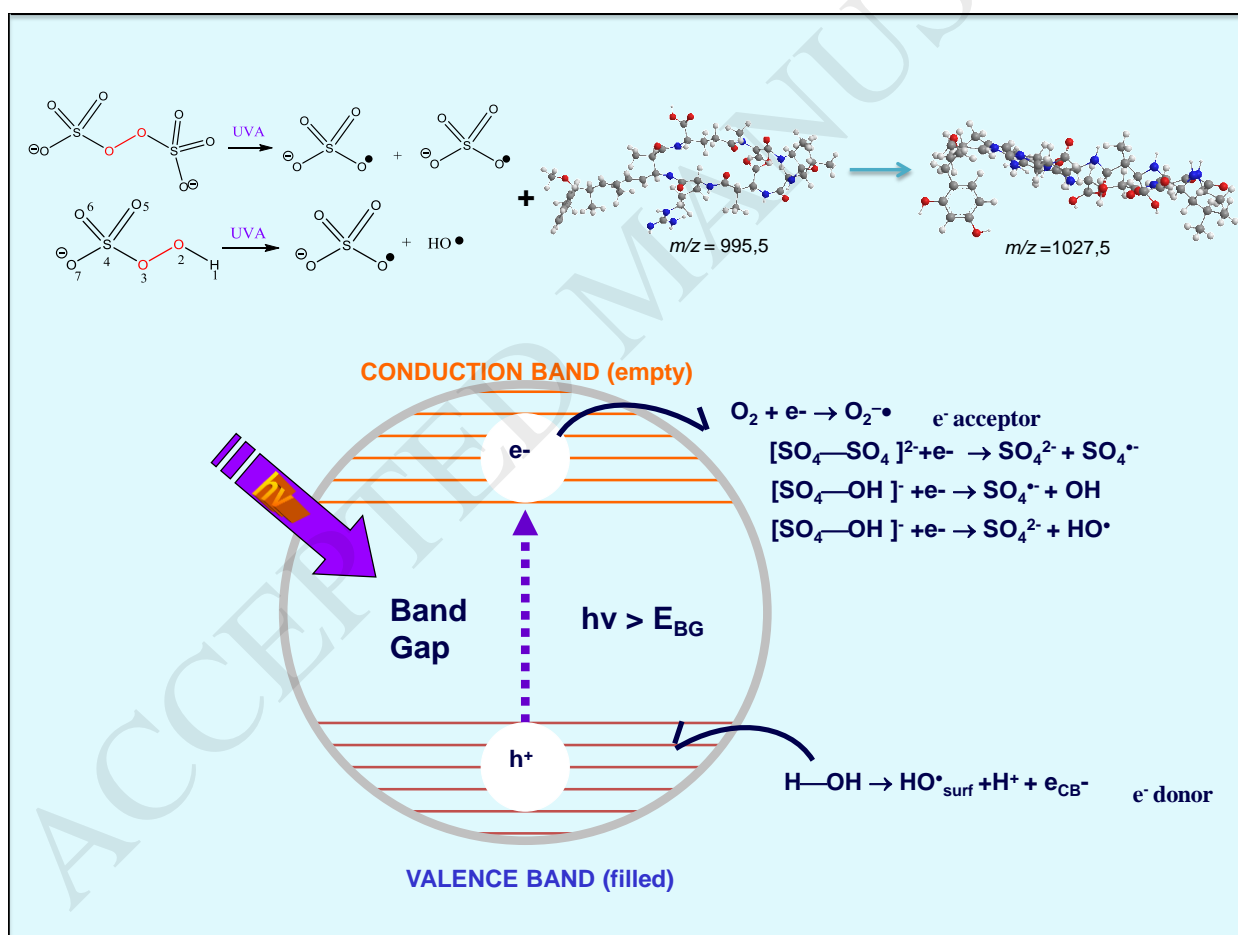
*<sup>4</sup>School of Pharmacy and Life Sciences, Robert Gordon University, Aberdeen, AB10 7GJ, UK.*

\*corresponding author email: maria,antoniou@cut.ac.cy

# Enhancing photocatalytic degradation of the cyanotoxin microcystin-LR with the addition of sulfate-radical generating oxidants

M.G. Antoniou, I. Boraie, M. Solakidou, Y. Deligiannakis, M. Abhishek, C. Edwards, and L.A. Lawton

## Graphic Abstract



## Highlights

- Investigation of sulfate radical generating oxidants with TiO<sub>2</sub> photocatalysis
- HSO<sub>5</sub><sup>-</sup> coupled with UVA/TiO<sub>2</sub> was the most energy efficient system
- Addition of oxidants prolonged the life-time of the formed radicals
- New intermediates based on consecutive hydroxyl substitutions of MC-LR were detected
- Toxicity studies on the treated samples indicated loss of MC-LR toxic properties

### Abstract

This study investigated the coupling of sulfate radical generating oxidants, (persulfate, PS and peroxymonosulfate, PMS) with TiO<sub>2</sub> photocatalysis for the degradation of microcystin-LR (MC-LR). Treatment efficiency was evaluated by estimating the electrical energy per order ( $E_{EO}$ ). Oxidant addition at 10 mg/L reduced the energy requirements of the treatment by 60% and 12% for PMS and PS, respectively compared with conventional photocatalysis. Quenching studies indicated that both sulfate and hydroxyl radicals contributed towards the degradation of MC-LR for both oxidants, while Electron Paramagnetic Resonance (EPR) studies confirmed that the oxidants prolonged that lifetime of both radicals (concentration maxima shifted from 10 to 20min), allowing for bulk diffusion and enhancing cyanotoxin removal. Structural identification of transformation products (TPs) formed during all treatments, indicated that early stage degradation of MC-LR occurred mainly on the aromatic ring and conjugated carbon double bonds of the ADDA amino acid. In addition, simultaneous hydroxyl substitution of the aromatic ring and the conjugated double carbon bonds of ADDA ( $m/z= 1027.5$ ) are reported for the first time. Oxidant addition also increased the rates of formation/degradation of TPs and affected the overall toxicity of the treated samples. The detoxification and degradation order of the treatments was UVA/TiO<sub>2</sub>/PMS > UVA/TiO<sub>2</sub>/PS >> UVA/TiO<sub>2</sub>.

**Keywords:** cyanotoxins, intermediates, TiO<sub>2</sub> photocatalysis, peroxymonosulfate, persulfate

## 1. Introduction

Cyanobacteria (blue-green algae) are well known for forming blooms (cyanobacterial harmful algal blooms, cyano-HABs) under suitable conditions, typically influenced by nutrients, light and temperature [1]. Such mass occurrences cause aesthetic, physical as well as taste and odor problems, however, their ability to produce and excrete toxic metabolites present a major hazard to human and animal health [1]. Hepatotoxic microcystins are undoubtedly the most commonly occurring toxins on a global basis and have been responsible for many animal and human toxicoses. They are, a large group of cyclic heptapeptides (249 variants) produced by a growing number of planktonic and benthic genera including *Microcystis*, *Anabaena*, *Nostoc*, *Planktothrix*, *Oscillatoria* [2, 3]. Among them, microcystin-LR (MC-LR where L is leucine and R is arginine) is the most toxic and most frequently detected variant in surface waters [1, 4]. Due to its acute and chronic toxicity, the World Health Organization (WHO) established a guideline of 1.0 µg/L as a maximum concentration of MC-LR in drinking water supplies [5].

The effects of climate change and anthropogenic activity are contributing to more frequent and prolonged blooms across the globe, adding further pressure on scarce fresh water supplies [6]. This is highlighted by an event in 2007, in Lake Taihu, China's third largest freshwater lake and sole water supply for the city of Wuxi, where >2 million people were without drinking water for over a week due to high concentrations of microcystins [7]. In 2014, a similar event occurred in Toledo, Ohio where drinking water contained 3 times the WHO guideline value of microcystin and led to a drinking water ban for several days [8].

In-lake treatment can be the first preventative measurement towards protecting human health from cyano-HABs [9], but there is still need for finding appropriate technologies for removing soluble cyanotoxins. An array of methods including conventional and emerging technologies has been tested for the removal of cyanotoxins. Conventional methods (coagulation, flocculation, rapid sand filtration) can remove cyanobacterial cells efficiently but have limited ability to remove cyanotoxins [10]. Therefore,

conventional chemical oxidation processes (chlorination, permanganate, UVC radiation) and advanced oxidation processes (AOPs) have been tested with various efficiencies [9, 11, 12].

Among the AOPs tested, titanium dioxide ( $\text{TiO}_2$ ) photocatalysis has been extensively studied for cyanotoxins removal, since it has shown potential not only for water purification but for detoxification without the formation of hazardous byproducts [9, 13-20]. The reactive oxygen species (ROS) formed during  $\text{TiO}_2$  photocatalysis include the hydroxyl radical ( $\text{HO}^\bullet$ ), superoxide anion radical ( $\text{O}_2^{\bullet-}$ ), hydroperoxyl radical ( $\text{HO}_2^\bullet$ ), singlet oxygen ( $^1\text{O}_2$ ), and their subsequent reactions with the target contaminants occur at or very near the  $\text{TiO}_2$  surface [21, 22]. Hydroxyl radicals, generated on the surface of the catalyst following oxidation of water from the positive holes of  $\text{TiO}_2$ , are non-selective oxidizing species with strong oxidation potential (+2.80V) that rapidly react with most organic compounds with rate constants in the order of  $10^6$ - $10^{10} \text{ M}^{-1} \text{ s}^{-1}$  [23]. Various studies have investigated the degradation of MC-LR in pure solutions or crude extracts with  $\text{TiO}_2$  photocatalysis to study the effect of specific water quality parameters [20, 24-26] or the properties of the photocatalyst used [18, 25, 27-30]. Solar light activated materials have also been tested to reduce application cost [19, 24, 27-29, 31]. Herein, sulfate radical generating oxidants were added as a way to reduce the energy requirements of the photocatalytic system for the removal of MC-LR as most of the light activated materials are not currently mass produced.

Sulfate radicals ( $\text{SO}_4^{\bullet-}$ ) are among the strongest oxidants known for the abstraction of electrons (2.5-3.1 V [32, 33]). They are much stronger than  $\text{HO}^\bullet$  radicals (1.89-2.72 V [23]) and other commonly used in the drinking water industry oxidants, such as permanganate ( $E = 1.70 \text{ V}$ ) (41) and hypochlorous acid ( $E = 1.49 \text{ V}$ ) [34]. Sulfate radicals can be produced through homolytic dissociation of the oxidants through heat and radiation and e- transfer mechanisms from Fenton-like reagents [35-37]. Neta et al. (1988) reported that owing to their selectivity, sulfate radicals are more efficient oxidants for the removal of organic compounds with unsaturated bonds and aromatic constituents than the hydroxyl radicals [33]. Yet there are limited studies on  $\text{SO}_4^{\bullet-}$ -based AOPs (compared with  $\text{HO}^\bullet$ ) for the degradation of recalcitrant organic contaminants and especially cyanotoxins [35, 38-40].

Even fewer studies have investigated the effect of coupling sulfate radical generating oxidants with TiO<sub>2</sub> on the removal of emerging contaminants with various light sources. Specifically, when low pressure UVA lamps were utilized in the UVA/TiO<sub>2</sub>/PS photocatalytic system for the removal of 2-chlorobiphenyl, the authors concluded that oxidant addition had a negative effect on contaminant removal [41]. When germicidal UV was used instead for catalyst and oxidant activation, in the UVC/TiO<sub>2</sub>/PS [42, 43] and UVC/TiO<sub>2</sub>/PMS [42] treatment, it was reported that oxidant addition in combination with TiO<sub>2</sub> significantly enhanced benzotriazole, humic acids, and heavy metals oxidation. Furthermore, simulated solar irradiation (SSI) has been used in the SSI/TiO<sub>2</sub>/PS treatment [44] and showed higher potential for the removal of the pesticide DEET compared with the SSI/TiO<sub>2</sub>/H<sub>2</sub>O<sub>2</sub> system. PS was also coupled with TiO<sub>2</sub> photocatalysts for the degradation of dyes under solar [45] and UV radiation [46].

With current research results being conflicting and the fact that, there are no other studies on coupling UVA/TiO<sub>2</sub> photocatalysis with sulfate radical generating oxidants (particularly PMS) for the removal of cyanotoxins, this study aimed to examine potential improvement of the photocatalytic efficiency of UVA/TiO<sub>2</sub> via the addition of sulfate radical generating oxidants, unveil degradation pathways, identify the radicals formed, and test for the toxicity of the treated samples. To the best of our knowledge, this is the first study that investigates the potential use of these oxidants coupled with UVA/TiO<sub>2</sub> for water purification and especially for the removal of the hepatotoxin microcystin-LR.

## 2. Materials and Methods

### 2.1 Reagents:

Microcystin-LR (MC-LR) standards were purified from batch cultures of *Microcystis aeruginosa* as previously described [47, 48]. A 500 mg/L stock solution of MC-LR was prepared by dissolving 1 mg of solid MC-LR (FW= 995.2 g/mole) with 2 mL of ELGA<sup>®</sup> water (resistivity = 18.2 MΩ conductivity = 0.05 μS/cm). Different toxin concentrations (5 mg/L and 10 mg/L) were achieved by spiking specific aliquots (range of μL) of the 500 mg/L standard solution in ELGA<sup>®</sup> water. Titanium dioxide (P25) was purchased

by Evonik Industries AG, Essen, Germany. The oxidants used in this study, potassium peroxymonosulfate (PMS,  $\text{HSO}_5^-$ ), potassium persulfate (PS,  $\text{K}_2\text{S}_2\text{O}_8$ ), and the quenching agent sodium thiosulfate ( $\text{Na}_2\text{S}_2\text{O}_3$ ) were purchased from Sigma-Aldrich (Poole, UK). OXONE<sup>®</sup> (95%, Dupont) is the commercial name of the triple-salt  $2\text{KHSO}_5 \cdot \text{KHSO}_4 \cdot \text{K}_2\text{SO}_4$  that releases PMS during dissociation. Stock solutions of 5.2 mM corresponding to 1000 mg/L of PS equivalent as active ingredient were freshly prepared in MQ- $\text{H}_2\text{O}$  since they have limited stability [35], while a solution of 0.1 g/L sodium thiosulfate was used to quench the samples from all the experiments where the oxidants were added.

## 2.2 Experimental set-up:

The experiments were conducted using 10 mL solutions in 30 mL borosilicate glass vials. A xenon UVA lamp (480W UVA Spot 400 Lamp with spectral output 330-450 nm, Dr. Hönle, Munich, Germany) was used to illuminate the reactor vessel from the side at a distance of 20 cm. The reaction solution was continuously stirred and oxygenated with air with a rate of 200  $\text{cm}^3/\text{min}$ . A cooling fan was used to control the reactor temperature ( $T = 32 \pm 3$  °C). For the treatment optimization experiments, samples (200  $\mu\text{L}$ ) were taken at specific time intervals and placed in 1.5 mL Eppendorf tubes. The samples were then centrifuged for 15 min at 13000 x g in a minispin centrifuge, (Eppendorf, UK) to remove the P25  $\text{TiO}_2$  nanoparticles and the supernatant was placed into 100  $\mu\text{L}$  glass inserts in 2 mL HPLC vials and analyzed for the remaining MC-LR by HPLC. For the experiments where oxidants were used, the samples were quenched with 200  $\mu\text{L}$  of 0.1 g/L sodium thiosulfate first and then handled as previously described. The solution pH was monitored at the beginning and completion of the experiments and was found to be stable at  $\text{pH} = 5.6 \pm 0.1$  for all the experiments. Raw water from the Clatto Water, Scotland, was spiked with MC-LR and treated with all described photocatalytic systems. The chemical properties of the raw water from Clatto were performed at James Hutten Institute, Aberdeen, UK (Table S1). For the investigation of transformation products (TPs), the initial toxin concentration was increased from 5 mg/L to 10 mg/L. When UVA/ $\text{TiO}_2$  was examined for TP formation, sampling was performed as described before and the samples were analyzed with UPLC/MS/MS. When oxidants were added for TPs identification, batch

experiments were conducted instead for each time point (the treated volume was 10 mL) and 10 mL of 0.1g/L  $\text{Na}_2\text{S}_2\text{O}_3$  were added to stop the oxidant from further reacting, the samples were first centrifuged (Haraeus Megafuge 40R, Thermo Scientific, UK) and then processed as described in Section 2.6.

### 2.3 Ferrioxalate Actinometry:

The intensity of the lamps was also measured with Potassium Ferrioxalate Actinometry [49]. The quantum yield of ferrous production at  $\lambda = 365$  nm is  $\phi_\lambda = 1.27 \pm 0.02$  [50]. The average light intensity from the lamps was  $(3.02 \pm 0.26) \cdot 10^{-8}$  Einstein/s. Based on the Planck–Einstein equation  $E = h \cdot c / \lambda$ , where  $h$  = Planck constant, the quantum energy that is contained by a photon at wavelength  $\lambda = 365$  nm is  $E_{365} = 5.44 \times 10^{-19}$  J/photon. Multiplication of  $E_{365}$  with the Avogadro's number transforms the units in  $E_{365} = 327,554$  J/Einstein [57]. The photon flux ( $P_{365}$ ) of the reactor is obtained by multiplying the estimated average irradiation with the quantum energy  $E_{365}$  and is equal to  $(9.88 \pm 0.85) \cdot 10^{-3}$  W.

### 2.4 HPLC Analysis:

MC-LR analysis was performed using Waters Alliance 2695 solvent delivery system with 2996 photodiode array detector (Waters, Elstree, UK). Samples were separated on Symmetry C18 Column (2.1 i.d. x 150 mm; 5  $\mu\text{m}$  particle size) maintained at 40°C. Eluent was monitored by UV absorption between 200-400 nm with detector resolution of 1.2 nm. The mobile phase constituted of ELGA® water (A) and acetonitrile (B) both containing 0.05% trifluoroacetic acid (TFA). Samples were separated using a gradient increasing from 15% to 65% B over 25 min at a flow rate of 0.3 mL  $\text{min}^{-1}$ , followed by ramp up to 100% B then re-equilibration at 15% over the next 10 min. Data acquisition and processing were performed using Empower software (Version 2.0). MC-LR was quantified by external calibration using the range of 0.1– 10,0 mg/L (linear range). The method detection limit (MDL) was estimated by multiplying the standard deviation of multiple measurements of the lowest standard with the corresponding t-student for 99% confidence level, as described in 40 CFR Ch. I (7–1–11 Edition) document of the USEPA. The MDL for this method was 7  $\mu\text{g/L}$ .

## 2.5 Electron Paramagnetic Resonance (EPR) Experiments and Hydroxyl and Sulfate Radicals

### Trapping

EPR spectra were recorded with a Bruker ER200D spectrometer equipped with an Agilent 5310A frequency counter, operating at X- band (9.61 GHz). All EPR experiments were monitored through bespoke software based on Lab View. Samples were illuminated *in situ* inside the EPR cavity using a 450W Xe- lamp (Oriel 66929), equipped with a water IR cut-off filter. The photogeneration of hydroxyl and sulfate radicals produced under continuous solar light irradiation ( $\lambda > 240\text{nm}$ ) of aqueous suspensions of the photocatalysts, were determined by EPR spin-trapping using DMPO as a spin trap for both radicals. Kinetic runs were performed at room temperature (25 °C) by recording the EPR signal intensity in three capillaries (20  $\mu\text{L}$  each), inserted in a 5mm suprasil EPR tube. For the spin trapping, 10 mg/L  $\text{TiO}_2$  particles were premixed with 10 mg/L of oxidant (PS or PMS), 100 ppm of DMPO and irradiated *in situ* in the EPR cavity. The irradiation time was varied from 30 seconds up to 60 minutes to monitor the radical photoinduction kinetics. The photoreaction setup used was calibrated with P25  $\text{TiO}_2$  and spin quantification was done by using DPPH as a spin standard. This setup produces 100  $\mu\text{mol HO}^\bullet$  per gram of irradiated P25  $\text{TiO}_2$  [51]. Each experiment was performed in triplicates and the variation between each radical identification experiments was at 2  $\mu\text{mol spins/g TiO}_2$  for  $\text{OH}^\bullet$  radicals and 3  $\mu\text{mol spins/g TiO}_2$  for  $\text{SO}_4^{\bullet-}$  radicals.

## 2.6 Solid Phase Extraction of MC-LR's photocatalytic transformation products

The photocatalytic transformation products of MC-LR samples were concentrated using ISOLUTE ENV+ (100 mg; Biotage, Cardiff, UK) SPE columns on a vacuum manifold. The cartridges were conditioned with 10 mL of MeOH followed by 10 mL of ELGA® water. Samples obtained after photocatalysis were centrifuged at 4,000 x g for 20 min and the supernatants were applied to the conditioned cartridges. Subsequently, the cartridges were washed with 10 mL of ELGA® water and dried under vacuum for 5 min. After drying, the cartridge was eluted with 1.5 mL of 80% methanol and analysed using UPLC-MS.

## 2.7 UPLC/MS Analysis

Analysis of samples from the investigation of TPs formed with the three photocatalytic systems was performed using Acquity UPLC system with photodiode array (ACQUITY UPLC PDA) equipped with Tandem Quadruple Time of Flight (Xevo QToF) in series (Waters, Elstree, UK). Samples were separated on Acquity UPLC® BEH C18 column (2.1 i.d. x 100 mm; 1.7 µm particle size; Waters, UK) maintained at 40°C. Milli-Q water (A) and acetonitrile (B) both containing 0.1% Formic acid (FA) constituted the mobile phase. Samples were separated using a gradient increasing from 20% to 70% B at flow rate of 0.2 mL min<sup>-1</sup> over 10 min, followed by ramp up to 100% B and then re-equilibration over 20% for the next 5 min. Eluent was monitored by UV absorption between 200-400 nm with detector resolution of 1.2 nm. Mass spectrometry analysis were performed in positive ion electro-spray mode (ES<sup>+</sup>), scanning from *m/z* 50 to 2000 Da with a scan time of 0.25 s and inter-scan delay of 0.025 s. The capillary voltage was set at 3.3 kV and cone voltage at 25.0 V. The source and desolvation temperatures were set to 80 °C and 300 °C respectively. Flow rate for cone gas and desolvation gas were 50 and 400 L h<sup>-1</sup> respectively. Low voltage scans were acquired a 6 V and high voltage using a ramp from 25-40 V, providing parent ion and characteristic fragment data respectively. Sodium iodide (2 µg/µL in 50% aqueous propan-2-ol (v/v)) was used as the calibrant with leucine-enkephalin (0.5 mg/L in 50% aqueous methanol (v/v)) as the lockspray. Instrumental control, data acquisition and processing were achieved using MassLynx software (Version 4.1).

## 2.8 Protein Phosphatase Inhibition Assay

The toxicity of samples obtained after photocatalytic treatment of MC-LR with sulphate-radical producing oxidants (i.e., PMS and PS) was assessed using PP1 Inhibition Assay. This colorimetric assay measures the ability of the PP1 enzyme to dephosphorylation the phospho-substrate *p*-nitrophenyl phosphate (*p*NPP) which results in the release of phosphoric ions and the colorimetric compound, *p*-nitrophenol (yellow color). The production of the *p*-nitrophenol and consequently the activity of PP1 can be quantified

by measuring the solution absorption at  $\lambda = 405$  nm. A modified procedure of previously reported colorimetric assay was employed [52-54]. More info can be found in S.I.

## 2.9. Data processing

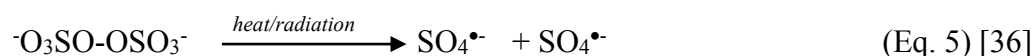
GraphPad Prism 5 software was utilized for the statistical analysis of the experimental data and for the calculation of the *EEo* values. The structures of the intermediates were drawn with the ChemBioDraw Ultra 13.0 software.

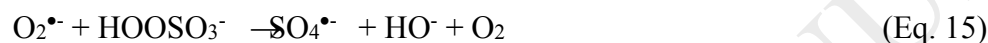
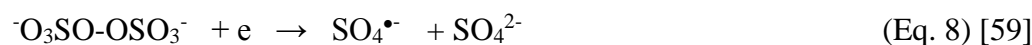
## 3. Results and Discussion

### 3.1 Effect of oxidants addition:

Once the optimum photocatalytic conditions were determined (Section S2.1), the effects of oxidant addition on TiO<sub>2</sub> photocatalysis were studied. The oxidants were added at a concentration of 0.052 mM corresponding to 10 mg/L of PS as active ingredient which was based on previous studies conducted by the authors [35]. Figure 1 summarizes the results from the addition of oxidants along with control experiments on the effect of UVA radiation alone, aeration, and UVA/Oxidant. UVA radiation alone had negligible effect on MC-LR removal as previously stated since the toxin has an adsorption maxima at  $\lambda = 238$  nm and negligible absorbance at  $\lambda = 365$  nm [14, 55]. Coupling of PS with UVA radiation resulted in a significant reduction of MC-LR ( $t=60$  min for  $C_{MCLR} < MDL$ ), while for equivalent concentrations of PMS treatment efficiency was significantly lower ( $t > 60$  min for  $C_{MCLR} < MDL$ ) [35]. However, when TiO<sub>2</sub> photocatalysis was coupled with the oxidants, UVA/TiO<sub>2</sub>/PMS had a more prominent effect on the energy requirements and treatment time than UVA/TiO<sub>2</sub>/PS ( $t = 5$  min and  $t = 10$  min for  $C_{MCLR} < MDL$ , respectively). In order to explain the differences on the efficiency of each treatment it is important to identify the type and mechanisms of ROS formed. Light activation of TiO<sub>2</sub> results in the formation of mainly hydroxyl radicals and the superoxide anion since the system was purged with air (Eq. 1-3) [22,

56]. Absence of aeration reduced photocatalytic degradation ( $t \sim 20$  min for  $C_{MCLR} < MDL$ ) (Figure 1). PS and PMS can undergo homolytic dissociation of the peroxide bond from radiation or thermal activation and give sulfate radicals, and sulfate and hydroxyl radicals, respectively (Eq. 4-5) [35]. The oxidants can also act as electron acceptors of the photo-excited electron from the conduction band of the  $TiO_2$  and through electron transfer mechanisms to give additional sulfate and hydroxyl radicals based on the reactions listed below (Eq. 6-8) [14, 57, 58]. Heat activation of oxidants did not contribute to radical formation because of the temperature in the reactor and the relatively short treatment times compared to what was reported needed in the literature [35]. On the other hand, homolytic dissociation of the peroxide bond of the oxidants through radiation seems to be a more probable mechanism. Even though, both oxidants have low absorption in the UVA range, the adsorption of PS at  $\lambda = 365$  nm is four times the one of PMS, when measured in solutions of the same concentration of active species [36]. This indicates that PS has a better ability to adsorb photons compared to PMS and therefore, more radicals can be formed. Moreover, the  $E_{EO}$  of the UVA/PS system was a third of the  $E_{EO}$  of UVA/PMS which means that the radicals formed with the UVA/PMS treatment are not reacting with the toxin but rather with each other (termination reactions) to form peroxides ( $H_2O_2$ ,  $S_2O_8^{2-}$ ) (Eq. 18, 21, 22) or with the remaining PMS (which is in excess compared to the toxin) and form peroxymonosulfate radicals ( $SO_5^{\bullet}$ ) (Eq. 11-12) that have significantly reduced oxidation ability and higher selectivity (redox potential 1.1 V, at pH = 7) to sulfate radicals. On the other hand, reaction of PS with a sulfate radical will cause the formation of another sulfate radical (Eq. 13) which leaves the oxidative capacity of the system unaltered.





When UVA/TiO<sub>2</sub> was coupled with sulfate radical generating oxidants for the removal of MC-LR, PMS reduced the  $E_{EO}$  by ~60% compared to conventional photocatalysis while PS had a slight reduction on the  $E_{EO}$  (~12%). During these treatments, all three previously mentioned radical formation mechanisms from the oxidants have contributed. Activation of oxidants through  $e^-$  transfer mechanisms (from the photoexcited  $e^-$  of the titania's conduction band (Eq. 6-8, 19) and the superoxide anion (Eq. 15-17, 20) appears to be the mechanism with the most significant contribution on radical formation in the

UVA/TiO<sub>2</sub>/Oxidant treatments. In general, the easiness which an e<sup>-</sup> is transferred to the lower unoccupied molecular orbital (LUMO) of peroxide oxidants is a measurement of its oxidizing properties [65]. Based on the LUMO properties of the oxidants their energy follows the order H<sub>2</sub>SO<sub>5</sub> < H<sub>2</sub>S<sub>2</sub>O<sub>8</sub> [65], which means, that PMS accepts e<sup>-</sup> more easily than PS and this may be the reason why it outperformed the latter when coupled with TiO<sub>2</sub> photocatalysis. To conclude the efficiency order of the tested treatment is UVA/TiO<sub>2</sub> < UVA/TiO<sub>2</sub>/PS < UVA/TiO<sub>2</sub>/PMS.

To test whether this order sustains under realistic treatment conditions, the three photocatalytic systems were applied to raw water from the Clatto reservoir in Dundee, Scotland. The water was first characterized for its chemical properties, spiked with MC-LR and then treated. Though the  $E_{EO}$  for all systems significantly increased, the efficiency order remained the same and UVA/TiO<sub>2</sub>/PMS has energy savings of 30 % vs 10% for UVA/TiO<sub>2</sub>/PS (Figure S4). Water matrix components such as TOC, alkalinity, and nitrogen-containing compounds are known to react competitively with MC-LR for radical utilization, which explains the five and ten fold increase of the  $E_{EO}$  compared to ELGA® water [24].

### 3.2 Radical identification:

The primary radicals formed from the enhanced photocatalytic systems can be potentially identified through the use of probes that selectively quench each type of radical [18, 42, 58]. The study of Fotiou and coworkers comprises a good example of use of such probes for the identification of ROS formed during UVA and visible light activated photocatalysts [18]. In this study, isopropanol (iPrOH) and tetrabutyl alcohol (TBA) were used as probes. Isopropanol can significantly scavenge hydroxyl radicals with a rate of  $k_{iPrOH,HR} = 1.9 \times 10^9 \text{ M}^{-1} \cdot \text{s}^{-1}$  [23] and sulfate radicals with rate  $k_{iPrOH,SR} = 8.0 \times 10^7 \text{ M}^{-1} \cdot \text{s}^{-1}$  [62]. In contrast, TBA scavenges hydroxyl radicals with rate of  $k_{TBA,HR} = 6.0 \times 10^8 \text{ M}^{-1} \cdot \text{s}^{-1}$  [23] whereas its scavenging rate for sulfate radical is 10<sup>3</sup> times less [42, 58]. Based on which probe has the biggest effect on the degradation rates of the target contaminant, it can be concluded whether one or both radicals have contributed to the degradation [42, 58]. Specifically, isopropanol can react with both types of radicals with the same rate, while TBA preferentially reacts with sulfate radicals. Persulfate radicals (SO<sub>5</sub><sup>•-</sup>), react

slowly with alcohols at rates  $<10^3 \text{ M}^{-1} \cdot \text{s}^{-1}$ , therefore their contribution to the degradation efficiency is considered negligible [33]. The probes were added to the UVA/TiO<sub>2</sub>/PS and UVA/TiO<sub>2</sub>/PMS systems at a [probe]/[oxidant]=10,000 molar ratio which was 10 times that of the cited literature [42, 58]. Based on the results of Figures S5 and S6 the addition of these probes did not give a clear indication on which type of radical contributed the most towards the degradation of MC-LR under our experimental conditions. This may be due to the fact that the previous studies quenched the effects of photocatalysts under various light sources or the oxidants but not their combination that tricks additional mechanisms for ROS formation.

It was therefore decided to use EPR spin-trapping that is eminently suited to selectively identify and quantify the photogeneration of hydroxyl and sulfate radicals [66]. The results depicted in Figure 2 represent the radicals formed during treatment with UVA/TiO<sub>2</sub>, UVA/TiO<sub>2</sub>/PS (Figure 2A), UVA/TiO<sub>2</sub>/PMS (Figure 2C), UVA/PS (Figure 2B), and UVA/PMS (Figure 2D). The amount of radicals formed with photocatalytic processes (conventional and enhanced) were significantly more than during photolysis of the oxidants. When UVA/TiO<sub>2</sub> was applied there was a sharp formation of short-lived hydroxyl radicals that peaked the first 10 min of irradiation and completed within the first 20 minutes treatment. On the other hand, when oxidants were added there was a continuous flow of radicals formed that had a delayed maxima between 20 and 30 minutes depending on the type of radical formed and oxidant used. This means that the presence of oxidants prolonged the lifetime of radicals, thus allowed for bulk diffusion and reaction with MC-LR. Since the treatment conditions chosen were not optimal for the toxin to adsorb onto the catalyst surface, the addition of oxidants not only compensated on that by providing additional radicals (quantitatively) but it also allowed for more radicals to reach the target molecule. Another interesting observation was that sulfate radicals were consistently detected at lower concentrations than hydroxyl, even during the homolytic dissociation of PS which generates only sulfate radicals. This means that a percentage of the formed sulfate radicals readily reacted with water to produce hydroxyl radicals (Eq.10). Moreover, the second order rate constant of this reaction is higher to the equivalent one of a hydroxyl radical producing a sulfate radical (Eq. 9). Based on the above and the data

depicted in Figures 2B & 2D, activation of PMS from the photo-excited  $e^-$  (and e-transfer mechanisms in general) results in the formation of sulfate radicals (Eq. 6 & Eq.15) because of the significant increase in the amount of sulfate radicals produced with the UVA/TiO<sub>2</sub>/PMS system vs. UVA/PMS.

### 3.3 Degradation pathways of MC-LR from conventional and enhanced photocatalysis:

Following the discussion in Section S2.2 on structural elucidation of the transformation products (TPs), the latter ones were organized into various degradation pathways. All the pathways and most of the proposed structures of the TPs were observed for all treatments, at varying rates of TP formation and degradation (Table S1).

1. MC-LR → Product 3A-C → Product 4A-C
2. MC-LR → Product 3D ↔ Product 3E
3. MC-LR → Product 2A → Product 1
4. MC-LR → Product 3F ↔ Product 3G  
                                   ↓                                  ↓  
                                   Product 4G ↔ Product 4H

The first pathway shows the single and double hydroxyl substitution of the aromatic ring, the second one the formation of enol-MC-LR ( $m/z$  1011.5, 3D) and its isomerization to the more stable tautomer ketone-MC-LR ( $m/z$  1011.5, 3E), while the third indicates how hydroxyl addition to the diene bonds can lead to the cleavage of part of the ADDA chain. The fourth pathway is believed to be mainly taking place during the TiO<sub>2</sub>/UVA/Oxidant treatment because more free radicals are available in the system that can attack any part of the toxin, even the ones that have increased shielding from the nearby functional groups. The double bond of the Mhda amino acid of the cyclic structure can go through hydroxyl substitution and the formation of the more stable ketone tautomer and the same time the aromatic ring of the ADDA amino acid can get hydroxylated. Since numerous TPs were detected it was important to ensure that treatment resulted in detoxification.

### 3.4 Inhibition studies based on the PP1 Enzyme

To assess the ability of the tested treatments to perform water detoxification, an assay based on the inhibition of protein phosphatase PP1 enzyme was employed [15] since microcystins are known for inhibiting PPs [67]. Standard solutions of MC-LR (3-1000  $\mu\text{g/L}$ ) were prepared to form the inhibition curve of the toxin with the PP1 enzyme (Figure S11). The 50<sup>th</sup> percentile of PP1 inhibition ( $\text{IC}_{50}$ ) was determined at 7.4  $\mu\text{g/L}$  of MC-LR. Due to the low  $\text{IC}_{50}$  determined, our method is considered highly sensitive. Samples from the conventional and enhanced photocatalysis, collected at different time points, were analyzed with the PP1 assay. Figure 3 depicts the percentage of the enzyme inhibition prior to treatment (control) and after allowing 5 min (Figure 3a) and 60 min (Figure 3b) of reaction time. The initial concentration of MC-LR used was sufficient to completely inhibit PP1. Application of UVA/ $\text{TiO}_2$  photocatalysis had a slight effect of the percentage of inhibition at the initial stages of degradation (Figure 3a), however by the end of treatment only a small percentage of the enzyme activity was still inhibited. UVA/ $\text{TiO}_2$ /PS exhibited similar behavior, however after the first 10 min of treatment (data not shown) the enzyme activity was recovered. The UVA/ $\text{TiO}_2$ /PMS was most successful with complete removal of toxicity after 5 min of treatment. Though, MC-LR removal was completed within 15 min, 10 min, and 5 min for UVA/ $\text{TiO}_2$ , UVA/ $\text{TiO}_2$ /PS, and UVA/ $\text{TiO}_2$ /PMS, respectively for UVA/ $\text{TiO}_2$  longer treatments were needed for detoxification. The amino acid in MC-LR that has been associated with its toxic properties (without itself being toxic) is the ADDA [67, 68]. As previously mentioned the TPs detected mainly involved alteration of the unsaturated carbon bonds of the ADDA, through hydroxylation and isomerization. These structural alterations may have caused reduction of toxicity because of changes in the hydrophobicity and orientation of the ADDA chain which hinders its proper binding with the PP1 enzyme [67, 68]. Towards the end of the treatment, the ADDA chain was cleaved ( $m/z = 835$ ) (at different rates based on the treatment applied, Table S1) and therefore no PP1 activity inhibition was observed.

#### 4. Conclusions

To conclude, the addition of the oxidant PMS and PS greatly enhanced the photocatalytic degradation of MC-LR and reduced the energy requirements of the photocatalytic reactor. Though PS showed higher

activation with UVA radiation alone, when coupled with TiO<sub>2</sub> photocatalysis, the UVA/TiO<sub>2</sub>/PMS treatment was found to be more energy efficient than the corresponding UVA/TiO<sub>2</sub>/PS treatment. The addition of oxidants initiated an array of side reactions that resulted in the formation of additional radical species from what are detected with conventional TiO<sub>2</sub> photocatalysis. EPR spectra revealed that the presence of both oxidants extended the life-time of ROS enabling them to continuously diffuse through the bulk layer and reach the target-cyanotoxin. Focusing on unveiling the initial stages of MC-LR degradation with conventional and enhanced photocatalysis, new transformation products with  $m/z = 1027.5$  were detected that correspond to two hydroxyl substitutions of the unsaturated carbon bonds of the toxin. Highly sensitive toxicity tests at the end of treatment proved complete water detoxification when oxidants were coupled with TiO<sub>2</sub> photocatalysis compared to conventional photocatalysis. The cost of electricity in EU for non-household use at 0,121 €/kWh [69], while the oxidant cost of 1.14 USD/kg for PS [70] and 1.30 USD/kg for PMS [71]. This means that addition of 10 mg/L equivalents of PS will have an extra cost for the facility of 1.6 \$cents/m<sup>3</sup> and 2.33 \$cents/m<sup>3</sup> water treated for PS and PMS, respectively, which is not prohibitive for treatment facilities considering the energy savings as seen in the case of Clatto WTW.

### **Acknowledgments**

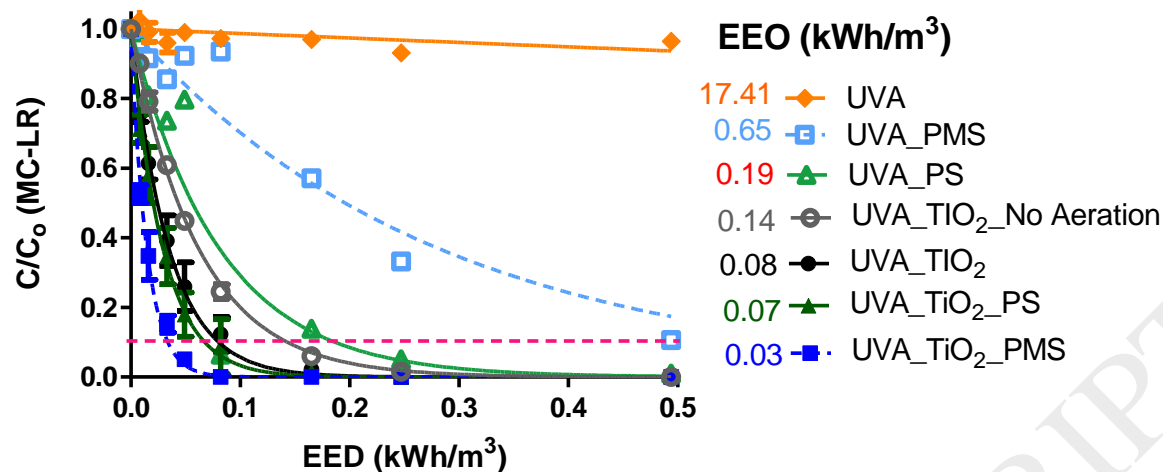
M.G.A is thankful to CUT for the funding through a start-up package (EX-90), the European Cooperation in Science and Technology, COST Action ES 1105 “CYANOCOST- Cyanobacterial blooms and toxins in water resources: Occurrence, impacts and management” for a Short Term Scientific Mission (STSM) grant, and the Erasmus Mobility Program. I.B. is thankful to the Erasmus Placement program for funding his term in RGU. The authors would like to thank C.M. Kyriakou (EST Department of CUT) for her assistance with part of the experiments.

### **Supplementary information**

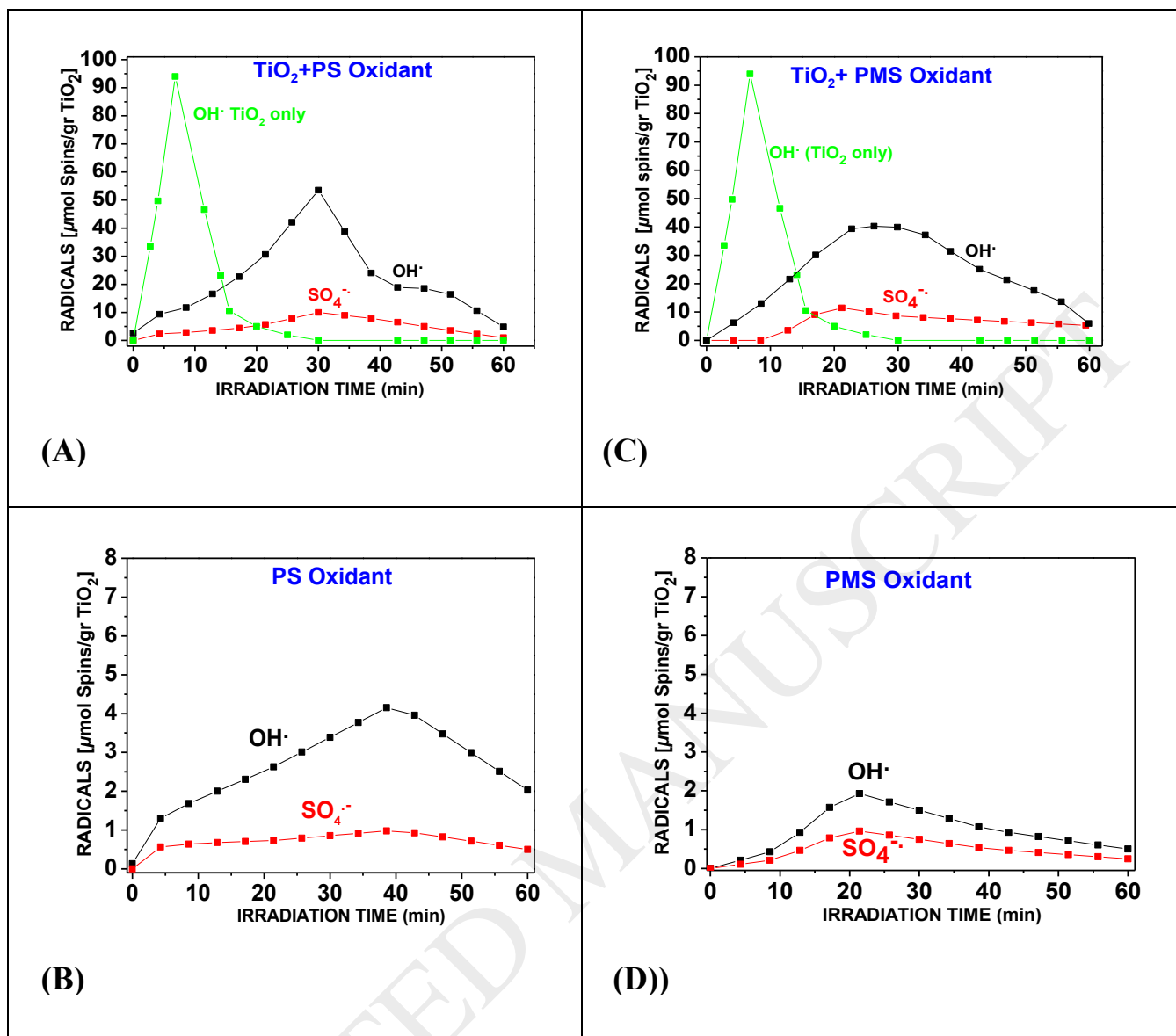
Supplementary data associated with this article can be found in a separate document.

ACCEPTED MANUSCRIPT

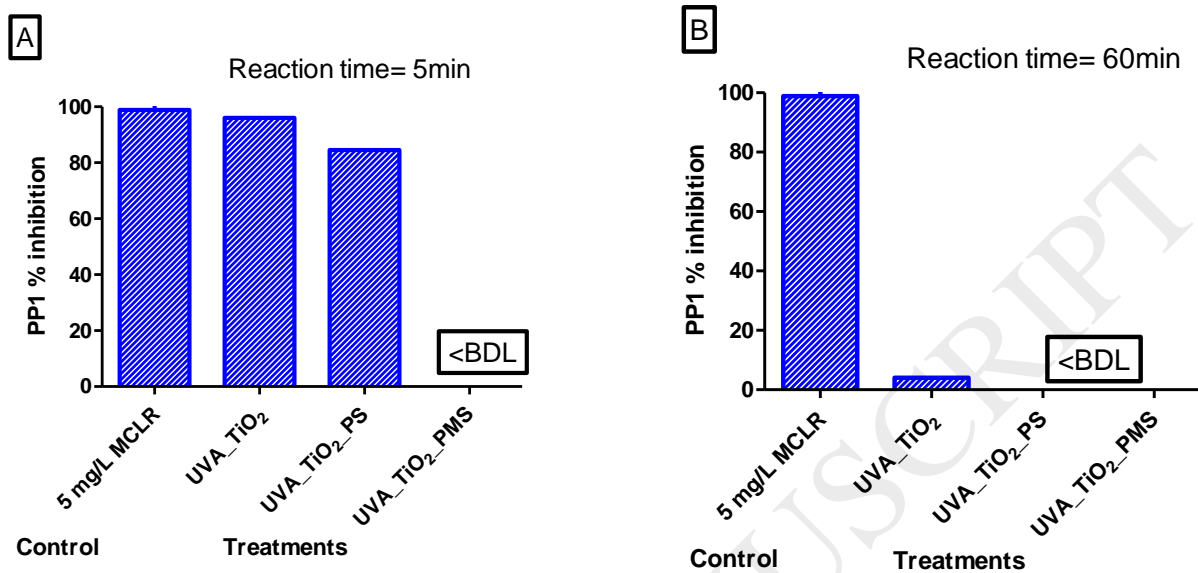
**Figures**



**Figure 1:** Degradation of 5 mg/L of MC-LR with various photocatalytic treatment processes based on the PS and PMS oxidant. (Experimental Conditions:  $P_{365} = 9.88$  mW, Oxidant 0.052 mM, TiO<sub>2</sub> 10 mg/L, pH<sub>SQ</sub> = 5.6, total treatment time shown = 30 min)



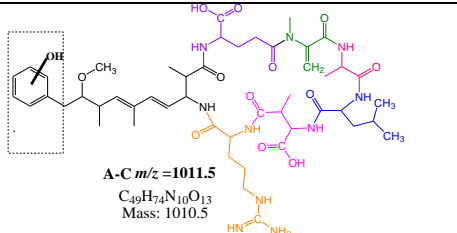
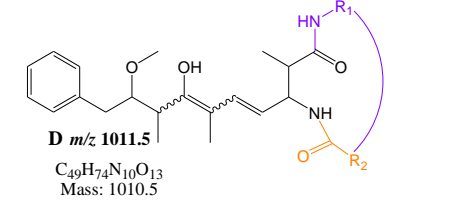
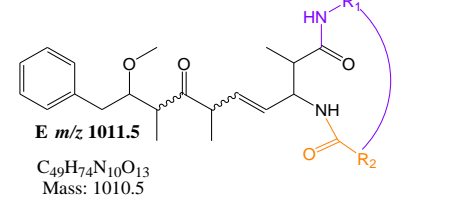
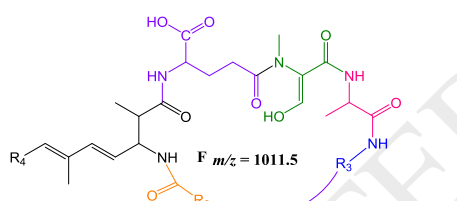
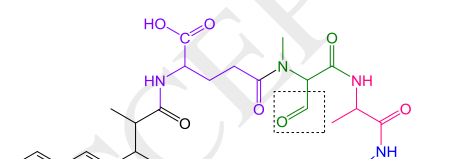
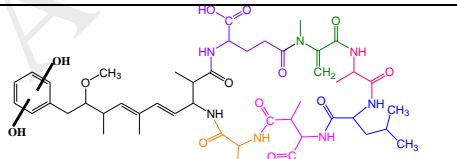
**Figure 2:** Photocatalytic generation of DMPO- $\text{OH}^\cdot$  (black squares), DMPO- $\text{SO}_4^{\cdot-}$  (red squares) radicals as a function of time with: A) UVA/ $\text{TiO}_2$ /PS, B) UVA/PS, C) UVA/ $\text{TiO}_2$ /PMS, and D) UVA/PMS.

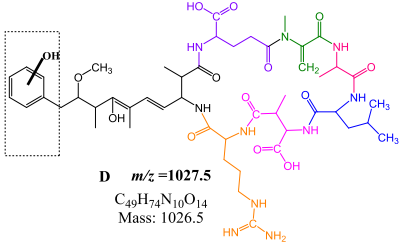
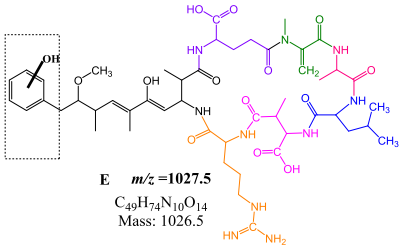
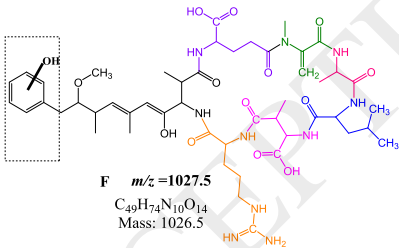
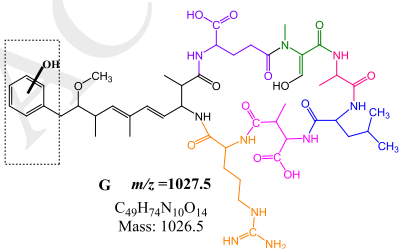


**Figure 3:** Effect of treatment type on the overall sample toxicity following (a) 5 min and (b) 60min of reaction time. (Experimental Conditions:  $C_0 = 10$  mg/L,  $P_{365} = 9.88$  mW, PS 0.052 mM, PMS 0.052 mM,  $TiO_2$  10 mg/L,  $pH_{SQ} = 5.6$ )

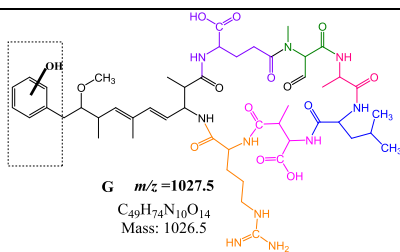
Table 1: Structures of reaction intermediates of MC-LR with TiO<sub>2</sub> based photocatalyst

No	Structure	m/z	Compound	Other Technologies	Reference
MCLR		995.5	C <sub>49</sub> H <sub>74</sub> N <sub>10</sub> O <sub>12</sub>	-	-
1	<p><i>m/z</i> 835.4 C<sub>37</sub>H<sub>58</sub>N<sub>10</sub>O<sub>12</sub> Mass: 834.4</p>	835.4	C <sub>37</sub> H <sub>58</sub> N <sub>10</sub> O <sub>12</sub>	TiO <sub>2</sub> <sub>p</sub> /UVA [72] TiO <sub>2</sub> <sub>f</sub> /UVA [55] NTiO <sub>2</sub> <sub>p</sub> /UVA [27] NFTiO <sub>2</sub> <sub>f</sub> /λ>420nm [29] PS/UVA [38] GO-TiO <sub>2</sub> /solar [19]	
2A	<p><b>A</b> <i>m/z</i> 1029.5 C<sub>49</sub>H<sub>76</sub>N<sub>10</sub>O<sub>14</sub> Mass: 1028.6</p>	1029.5	C <sub>49</sub> H <sub>76</sub> N <sub>10</sub> O <sub>14</sub>	TiO <sub>2</sub> <sub>p</sub> /UVA [72] TiO <sub>2</sub> <sub>f</sub> /UVA [55]# NTiO <sub>2</sub> <sub>p</sub> /λ>420nm [27] NTiO <sub>2</sub> <sub>p</sub> /UVA [27] NFTiO <sub>2</sub> <sub>f</sub> /λ>420nm [29] PS/UVA [38]# GO-TiO <sub>2</sub> /solar [19][43]	
2B	<p><b>B</b> <i>m/z</i> 1029.5 C<sub>49</sub>H<sub>76</sub>N<sub>10</sub>O<sub>14</sub> Mass: 1028.6</p>				
2C	<p><b>C</b> <i>m/z</i> 1029.5 C<sub>49</sub>H<sub>76</sub>N<sub>10</sub>O<sub>14</sub> Mass: 1028.6</p>				
2D	<p><b>D</b> <i>m/z</i> = 1029.5</p>				

3A 3B 3C	 <p><b>A-C</b> <math>m/z = 1011.5</math>  <math>C_{49}H_{74}N_{10}O_{13}</math>  Mass: 1010.5</p>	1011.5	$C_{49}H_{74}N_{10}O_{13}$	$TiO_2\_f/UVA$ $NFTiO_2\_f/\lambda > 420nm$ PS/UVA GO- $TiO_2$ /solar	[72] <sup>#</sup> [29] [38] <sup>#</sup> [19]
3D	 <p><b>D</b> <math>m/z</math> 1011.5  <math>C_{49}H_{74}N_{10}O_{13}</math>  Mass: 1010.5</p>				
3E	 <p><b>E</b> <math>m/z</math> 1011.5  <math>C_{49}H_{74}N_{10}O_{13}</math>  Mass: 1010.5</p>				
3F	 <p><b>F</b> <math>m/z = 1011.5</math></p>				
3G	 <p><b>G</b> <math>m/z = 1011.5</math></p>				
4A 4B 4C	 <p><math>m/z = 1027.5</math>  <math>C_{49}H_{74}N_{10}O_{14}</math>  Mass: 1026.5</p>	1027.5	$C_{49}H_{74}N_{10}O_{14}$	$TiO_2\_f/UVA$ $NFTiO_2\_f/\lambda > 420nm$ PS/UVA GO- $TiO_2$ /solar	[72] [29] [38] [19]

4D	 <p><b>D</b> <math>m/z = 1027.5</math>  <math>C_{49}H_{74}N_{10}O_{14}</math>  Mass: 1026.5</p>	1027.5	$C_{49}H_{74}N_{10}O_{14}$	N/A	N/A
4E	 <p><b>E</b> <math>m/z = 1027.5</math>  <math>C_{49}H_{74}N_{10}O_{14}</math>  Mass: 1026.5</p>				
4F	 <p><b>F</b> <math>m/z = 1027.5</math>  <math>C_{49}H_{74}N_{10}O_{14}</math>  Mass: 1026.5</p>				
4G	 <p><b>G</b> <math>m/z = 1027.5</math>  <math>C_{49}H_{74}N_{10}O_{14}</math>  Mass: 1026.5</p>				

4H



TiO<sub>2</sub>\_p = TiO<sub>2</sub> particles

TiO<sub>2</sub>\_f = TiO<sub>2</sub> films

# Displayed structures A-D were observed by [38] or [55].

**References:**

- [1] W.W. Carmichael, The toxins of cyanobacteria., *Sci. Am.* 270 (1994) 78-86.
- [2] R.W. Zurawell, H. Chen, J.M. Burke, E.E. Prepas, Hepatotoxic cyanobacteria: A review of the biological importance of microcystins in freshwater environments, *J. Toxicol. Environ. Health Part B.* 8 (2005) 1-37.
- [3] J. Meriluoto, L. Spoof, G.A. Codd, *Handbook of Cyanobacterial Monitoring and Cyanotoxin Analysis*, 1 ed., Wiley, 2017.
- [4] A.A. de la Cruz, M.G. Antoniou, A. Hiskia, M. Pelaez, W. Song, K.E. O'Shea, X. He, D.D. Dionysiou, Can we effectively degrade microcystins? - implications on human health, *Anti-Cancer Agents in Medicinal Chemistry.* 11 (2011) 19-37.
- [5] WHO, *Guidelines for drinking water quality*, 2nd ed. Addendum to vol. 2. Health criteria and other supporting information. World Health Organization, Geneva: 95-110 (2008).
- [6] H.W. Paerl, V.J. Paul, Climate change: Links to global expansion of harmful cyanobacteria, *Water Res.* 46 (2012) 1349-1363.
- [7] B. Qin, G. Zhu, G. Gao, Y. Zhang, W. Li, H.W. Paerl, W.W. Carmichael, A drinking water crisis in Lake Taihu, China: Linkage to climatic variability and lake management, *Environ. Manage.* 45 (2010) 105-112.
- [8] M.J. Harke, T.W. Davis, S.B. Watson, C.J. Gobler, Nutrient-Controlled Niche Differentiation of Western Lake Erie Cyanobacterial Populations Revealed via Metatranscriptomic Surveys, *Environ. Sci. Technol.* 50 (2016) 604-615.
- [9] M.G. Antoniou, A.A. de La Cruz, M.A. Pelaez, C. Han, X. He, D.D. Dionysiou, W. Song, K. O'Shea, L. Ho, G. Newcombe, M.B. Dixon, M.R. Teixeira, T.M. Triantis, A. Hiskia, T. Kaloudis, R. Balasubramanian, S. Pavagadhi, V.K. Sharma, Practices that Prevent the Formation of Cyanobacterial Blooms in Water Resources and Remove Cyanotoxins During Physical Treatment of Drinking Water, in: S. Ahuja (Ed.), *Comprehensive Water Quality and Purification*, Volume 2, Elsevier, United States of America, 2014, pp. 173-195.
- [10] M.G. Antoniou, A.A. de la Cruz, D.D. Dionysiou, Cyanotoxins: New generation of water contaminants, *J. Environ. Eng.* 131 (2005) 1239-1243.
- [11] L.A. Lawton, P.K.J. Robertson, Physico-chemical treatment methods for the removal of microcystins (cyanobacterial hepatotoxins) from potable waters, *Chem. Soc. Rev.* 28 (1999) 217-224.
- [12] V.K. Sharma, T.M. Triantis, M.G. Antoniou, X. He, M. Pelaez, C. Han, W. Song, K.E. O'Shea, A.A. De La Cruz, T. Kaloudis, A. Hiskia, D.D. Dionysiou, Destruction of microcystins by conventional and advanced oxidation processes: A review, *Separation and Purification Technology.* 91 (2012) 3-17.
- [13] A. Hiskia, T.M. Triantis, M.G. Antoniou, A.A. De La Cruz, K.E. O'Shea, W. Song, T. Fotiou, T. Kaloudis, J. Andersen, D.D. Dionysiou, Destruction of microcystins by conventional and advanced oxidation processes: A review, in: D.A. Lambropoulou, L.A.L. Nollet (Eds.), *Transformation Products of Emerging Contaminants in the Environment: Analysis, Processes, Occurrence, Effects and Risks*, JohnWiley & Sons, Ltd, 2014, pp. 687-720.

- [14] M.G. Antoniou, P.A. Nicolaou, J.A. Shoemaker, A.A. de la Cruz, D.D. Dionysiou, Impact of the morphological properties of thin TiO<sub>2</sub> photocatalytic films on the detoxification of water contaminated with the cyanotoxin, microcystin-LR, *Applied Catalysis B: Environmental*. 91 (2009) 165-173.
- [15] I. Liu, L.A. Lawton, B. Cornish, P.K.J. Robertson, Mechanistic and toxicity studies of the photocatalytic oxidation of microcystin-LR, *J. Photochem. Photobiol. A*. 148 (2002) 349-354.
- [16] C.J. Pestana, C. Edwards, R. Prabhu, P.K.J. Robertson, L.A. Lawton, Photocatalytic degradation of eleven microcystin variants and nodularin by TiO<sub>2</sub> coated glass microspheres, *J. Hazard. Mater.* 300 (2015) 347-353.
- [17] T. Fotiou, T.M. Triantis, T. Kaloudis, A. Hiskia, Evaluation of the photocatalytic activity of TiO<sub>2</sub> based catalysts for the degradation and mineralization of cyanobacterial toxins and water off-odor compounds under UV-A, solar and visible light, *Chem. Eng. J.* 261 (2015) 17-26.
- [18] T. Fotiou, T.M. Triantis, T. Kaloudis, K.E. O'Shea, D.D. Dionysiou, A. Hiskia, Assessment of the roles of reactive oxygen species in the UV and visible light photocatalytic degradation of cyanotoxins and water taste and odor compounds using C-TiO<sub>2</sub>, *Water Res.* 90 (2016) 52-61.
- [19] T. Fotiou, T.M. Triantis, T. Kaloudis, L.M. Pastrana-Martínez, V. Likodimos, P. Falaras, A.M.T. Silva, A. Hiskia, Photocatalytic degradation of microcystin-LR and off-odor compounds in water under UV-A and solar light with a nanostructured photocatalyst based on reduced graphene oxide-TiO<sub>2</sub> composite. Identification of intermediate products., *Industrial and Engineering Chemistry Research*. 52 (2013) 13991-14000.
- [20] A.J. Feitz, T.D. Waite, G.J. Jones, B.H. Boyden, P.T. Orr, Photocatalytic degradation of the blue green algal toxin microcystin-LR in a natural organic-aqueous matrix, *Environmental Science and Technology*. 33 (1999) 243-249.
- [21] P. Pichat, A brief overview of photocatalytic mechanisms and pathways in water, *Water Science and Technology*. 55 (2007) 167-173.
- [22] M.R. Hoffmann, S.T. Martin, W. Choi, D.W. Bahnemann, Environmental applications of semiconductor photocatalysis, *Chem. Rev.* 95 (1995) 69-96.
- [23] G.V. Buxton, C.L. Greenstock, W.P. Helman, A.B. Ross, Critical review of rate constants for reactions of hydrated electrons, hydrogen atoms and hydroxyl radicals in aqueous solution, *J.Phys.Chem.Ref.Data*. 17 (1988) 513-886.
- [24] M. Pelaez, A.A. de la Cruz, K. O'Shea, P. Falaras, D.D. Dionysiou, Effects of water parameters on the degradation of microcystin-LR under visible light-activated TiO<sub>2</sub> photocatalyst, *Water Res.* 45 (2011) 3787-3796.
- [25] P.K.J. Robertson, L.A. Lawton, B. Münch, J. Rouzade, Destruction of cyanobacterial toxins by semiconductor photocatalysis, *Chemical Communications* (1997) 393-394.
- [26] L.A. Lawton, P.K.J. Robertson, B.J.P.A. Cornish, I.L. Marr, M. Jaspars, Processes influencing surface interaction and photocatalytic destruction of microcystins on titanium dioxide photocatalysts, *J. Catal.* 213 (2003) 109-113.

- [27] H. Choi, M.G. Antoniou, M. Pelaez, A.A. De La Cruz, J.A. Shoemaker, D.D. Dionysiou, Mesoporous nitrogen-doped TiO<sub>2</sub> for the photocatalytic destruction of the cyanobacterial toxin microcystin-LR under visible light irradiation, *Environmental Science and Technology*. 41 (2007) 7530-7535.
- [28] M. Pelaez, P. Falaras, V. Likodimos, A.G. Kontos, A.A. de la Cruz, K. O'shea, D.D. Dionysiou, Synthesis, structural characterization and evaluation of sol-gel-based NF-TiO<sub>2</sub> films with visible light-photoactivation for the removal of microcystin-LR, *Applied Catalysis B: Environmental*. 99 (2010) 378-387.
- [29] J. Andersen, C. Han, K. O'Shea, D.D. Dionysiou, Revealing the degradation intermediates and pathways of visible light-induced NF-TiO<sub>2</sub> photocatalysis of microcystin-LR, *Applied Catalysis B: Environmental*. 154-155 (2014) 259-266.
- [30] T. Fotiou, T.M. Triantis, T. Kaloudis, A. Hiskia, Evaluation of the photocatalytic activity of TiO<sub>2</sub> based catalysts for the degradation and mineralization of cyanobacterial toxins and water off-odor compounds under UV-A, solar and visible light, *Chem. Eng. J.* (2014).
- [31] M. Pelaez, P. Falaras, A.G. Kontos, A.A. De la Cruz, K. O'shea, P.S.M. Dunlop, J.A. Byrne, D.D. Dionysiou, A comparative study on the removal of cylindrospermopsin and microcystins from water with NF-TiO<sub>2</sub>-P25 composite films with visible and UV-vis light photocatalytic activity, *Applied Catalysis B: Environmental*. 121-122 (2012) 30-39.
- [32] L. Ebersson, Electron-Transfer Reactions in Organic Chemistry, *Adv. Phys. Org. Chem.* 18 (1982) 79-185.
- [33] P. Neta, R.E. Huie, A.B. Ross, Rate constants for reactions of inorganic radicals in aqueous solution, *J.Phys.Chem.Ref.Data*. 17 (1988) 1027-1284.
- [34] O. Legrini, E. Oliveros, A.M. Braun, Photochemical processes for water treatment, *Chem. Rev.* 93 (1993) 671-698.
- [35] M.G. Antoniou, A.A. de la Cruz, D.D. Dionysiou, Degradation of microcystin-LR using sulfate radicals generated through photolysis, thermolysis and e<sup>-</sup> transfer mechanisms, *Applied Catalysis B: Environmental*. 96 (2010) 290-298.
- [36] G.P. Anipsitakis, D.D. Dionysiou, Transition metal/UV-based advanced oxidation technologies for water decontamination, *Applied Catalysis B: Environmental*. 54 (2004) 155-163.
- [37] G.P. Anipsitakis, D.D. Dionysiou, M.A. Gonzalez, Cobalt-mediated activation of peroxymonosulfate and sulfate radical attack on phenolic compounds. Implications of chloride ions, *Environmental Science and Technology*. 40 (2006) 1000-1007.
- [38] M.G. Antoniou, A.A. De La Cruz, D.D. Dionysiou, Intermediates and reaction pathways from the degradation of microcystin-LR with sulfate radicals, *Environmental Science and Technology*. 44 (2010) 7238-7244.
- [39] X. He, A.A. de la Cruz, A. Hiskia, T. Kaloudis, K. O'Shea, D.D. Dionysiou, Destruction of microcystins (cyanotoxins) by UV-254 nm-based direct photolysis and advanced oxidation processes (AOPs): Influence of variable amino acids on the degradation kinetics and reaction mechanisms, *Water Res.* 74 (2015) 227-238.

- [40] X. He, A.A. de la Cruz, K.E. O'Shea, D.D. Dionysiou, Kinetics and mechanisms of cylindrospermopsin destruction by sulfate radical-based advanced oxidation processes, *Water Res.* 63 (2014) 168-178.
- [41] Y. Wang, C. Hong, Effect of hydrogen peroxide, periodate and persulfate on photocatalysis of 2-chlorobiphenyl in aqueous TiO<sub>2</sub> suspensions, *Water Res.* 33 (1999) 2031-2036.
- [42] M. Ahmadi, F. Ghanbari, M. Moradi, Photocatalysis assisted by peroxymonosulfate and persulfate for benzotriazole degradation: effect of pH on sulfate and hydroxyl radicals, *Water Science & Technology.* 72 (2015) 2095-2102.
- [43] J.T. Jung, J.Y. Choi, J. Chung, Y.W. Lee, J.O. Kim, UV/TiO<sub>2</sub> and UV/TiO<sub>2</sub>/chemical oxidant processes for the removal of humic acid, Cr and Cu in aqueous TiO<sub>2</sub> suspensions, *Environmental technology.* 30 (2009) 225-232.
- [44] M. Antonopoulou, I.K. Konstantinou, Effect of oxidants in the photocatalytic degradation of DEET under simulated solar irradiation in aqueous TiO<sub>2</sub> suspensions, *Global NEST Journal.* 16 (2014) 507-515.
- [45] V. Augugliaro, C. Baiocchi, A.B. Prevot, E. García-López, V. Loddo, S. Malato, G. Marci, L. Palmisano, M. Pazzi, E. Pramauro, Azo-dyes photocatalytic degradation in aqueous suspension of TiO<sub>2</sub> under solar irradiation, *Chemosphere.* 49 (2002) 1223-1230.
- [46] M. Saquib, M. Muneer, TiO<sub>2</sub>/mediated photocatalytic degradation of a triphenylmethane dye (gentian violet), in aqueous suspensions, *Dyes Pigm.* 56 (2003) 37-49.
- [47] C. Edwards, L.A. Lawton, S.M. Coyle, P. Ross, Laboratory-scale purification of microcystins using flash chromatography and reversed-phase high-performance liquid chromatography, *J. Chromatogr. A.* 734 (1996) 163-173.
- [48] C. Edwards, L.A. Lawton, Assessment of microcystin purity using charged aerosol detection, *J. Chromatogr. A.* 1217 (2010) 5233-5238.
- [49] S.L. Murov, I. Carmichael, G.L. Hug, *Handbook of Photochemistry*, 2nd ed. (revised and expanded), Marcel Dekker, New York, 1993, pp. 298-305.
- [50] S. Goldstein, J. Rabani, The ferrioxalate and iodide-iodate actinometers in the UV region, *J. Photochem. Photobiol. A Chem.* 193 (2008) 50-55.
- [51] Y. Kanigaridou, A. Petala, Z. Frontistis, M. Antonopoulou, M. Solakidou, I. Konstantinou, Y. Deligiannakis, D. Mantzavinos, D.I. Kondarides, Solar photocatalytic degradation of bisphenol A with CuO<sub>x</sub>/BiVO<sub>4</sub>: Insights into the unexpectedly favorable effect of bicarbonates, *Chem. Eng. J.* 318 (2017) 39-49.
- [52] W.W. Carmichael, J. An, Using an enzyme linked immunosorbent assay (ELISA) and a protein phosphatase inhibition assay (PPIA) for the detection of microcystins and nodularins, *Nat. Toxins.* 7 (1999) 377-385.
- [53] J. An, W.W. Carmichael, Use of a colorimetric protein phosphatase inhibition assay and enzyme linked immunosorbent assay for the study of microcystins and nodularins, *Toxicon.* 32 (1994) 1495-1507.

- [54] C.J. Ward, K.A. Beattie, E.Y.C. Lee, G.A. Codd, Colorimetric protein phosphatase inhibition assay of laboratory strains and natural blooms of cyanobacteria: Comparisons with high-performance liquid chromatographic analysis for microcystins, *FEMS Microbiol. Lett.* 153 (1997) 465-473.
- [55] M.G. Antoniou, J.A. Shoemaker, A.A. De La Cruz, D.D. Dionysiou, Unveiling new degradation intermediates/pathways from the photocatalytic degradation of microcystin-LR, *Environmental Science and Technology.* 42 (2008) 8877-8883.
- [56] P. Pichat, C. Guillard, C. Maillard, L. Amalric, J.C. D'Oliveira, TiO<sub>2</sub> photocatalytic destruction of water aromatic pollutants: Intermediates; properties degradability correlation; effects of inorganic ions and TiO<sub>2</sub> surface area; comparisons with H<sub>2</sub>O<sub>2</sub> processes, in: D.F. Ollis, H. AIEkabi (Eds.), *Photocatalytic Purification and Treatment of Water and Air*, Elsevier, Amsterdam, The Netherlands, 1993, pp. 207-223.
- [57] I.K. Konstantinou, T.A. Albanis, TiO<sub>2</sub>-assisted photocatalytic degradation of azo dyes in aqueous solution: Kinetic and mechanistic investigations: A review, *Appl. Catal. B Environ.* 49 (2004) 1-14.
- [58] G.P. Anipsitakis, D.D. Dionysiou, Degradation of organic contaminants in water with sulfate radicals generated by the conjunction of peroxymonosulfate with cobalt, *Environmental Science and Technology.* 37 (2003) 4790-4797.
- [59] B.C. Gilbert, J.K. Stell, Mechanisms of peroxide decomposition. An ESR study of the reactions of the peroxomonosulphate anion (HOOSO<sub>3</sub><sup>-</sup>) with TiIII, FeII, and a-oxygen-substituted radicals, *Journal of the Chemical Society, Perkin Transactions 2* (1990) 1281-1288.
- [60] D.G. Marketos, Rate Constants for Some Reactions of the OH Radical in Irradiated Aqueous Solutions at Different pH Values, *Z. Phys. Chem.* 65 (1969) 306-321.
- [61] A.K. Pikaev, V.I. Zolotarevskii, Pulse radiolysis of aqueous solutions of sulfuric acid, *Russ Chem Bull.* 16 (1967) 181-182.
- [62] A.B. Ross, P. Neta, RATE CONSTANTS FOR REACTIONS OF INORGANIC RADICALS IN AQUEOUS SOLUTION., *Natl Bur Stand Natl Stand Ref Data Ser* (1979).
- [63] R.C. Thompson, Catalytic decomposition of peroxymonosulfate in aqueous perchloric acid by the dual catalysts Ag<sup>+</sup> and S<sub>2</sub>O<sub>8</sub><sup>2-</sup> and by Co<sup>2+</sup>, *Inorg. Chem.* 20 (1981) 1005-1010.
- [64] H. Lin, J. Wu, H. Zhang, Degradation of clofibric acid in aqueous solution by an EC/Fe<sup>3+</sup>/PMS process, *Chem. Eng. J.* 244 (2014) 514-521.
- [65] A.G. Miroshnichenko, V.A. Lunenok-Burmakina, A quantum-mechanical study of the structure of inorganic derivatives of hydrogen peroxide, *Theor Exp Chem.* 11 (1976) 320-325.
- [66] G.M. Rosen, E. Finkelstein, Use of spin traps in biological systems, *Adv. Free Radic. Biol. Med.* 1 (1985) 345-375.
- [67] J. Goldberg, H. Huang -b., Y. Kwon -g., P. Greengard, A.C. Nairn, J. Kuriyan, Three-dimensional structure of the catalytic subunit of protein serine/threonine phosphatase-1, *Nature.* 376 (1995) 745-753.
- [68] K.I. Harada, S. Imanishi, H. Kato, M. Mizuno, E. Ito, K. Tsuji, Isolation of Adda from microcystin-LR by microbial degradation, *Toxicol.* 44 (2004) 107-109.

- [69] Eurostat. Statistics Explained, Electricity Prices Statistics. [http://ec.europa.eu/eurostat/statistics-explained/index.php/Electricity\\_price\\_statistics](http://ec.europa.eu/eurostat/statistics-explained/index.php/Electricity_price_statistics) (February 5, 2018).
- [70] M.G. Antoniou, H.R. Andersen, Comparison of UVC/S2O8<sup>2-</sup> with UVC/H2O2 in terms of efficiency and cost for the removal of micropollutants from groundwater, *Chemosphere*. 119 (2015) S81-S88.
- [71] E.L. Springer, Potential uses for peroxymonosulfate in pulping and bleaching, *Proceedings of the 1989 and 1990 AIChE Forest Products Symposium* (1992) 113-120.
- [72] I. Liu, L.A. Lawton, P.K.J. Robertson, Mechanistic studies of the photocatalytic oxidation of microcystin-LR: An investigation of byproducts of the decomposition process, *Environmental Science and Technology*. 37 (2003) 3214-3219.

ACCEPTED MANUSCRIPT